PHOTONICSGAIN-0D SOLVER AT NANOHUB: DESCRIPTION

LUDMILA PROKOPEVA, ALEXANDER KILDISHEV, NIKITA ARNOLD, 11/2012

NOTATIONS AND ACRONYMS

$c,\,\varepsilon_0,\,\mu_0$ – speed of light, permittivity and permeability in vacuum in SI units

$\hbar$ – reduced Planck constant, [J·s]

E_i – energy of i -th level, [J]

N_{tot} – the conserved total population density, $[\mathrm{m}^{-3}]$

$\tau_{\mathrm{r},ij}$, $\tau_{\mathrm{nr},ij}$, $\tau_{ij}=(\tau_{\mathrm{r},ij}^{-1}+\tau_{\mathrm{nr},ij}^{-1})^{-1}$ – radiative, non-radiative and total lifetimes of the transition ij, [s]

ω_{ij}, Γ_{ij}, ϕ_{ij} – Lorentzian resonant frequency [rad/s], damping constant [1/s], and phase shift [rad]

$\lambda_{ij}=2\pi c\omega_{ij}^{-1}$ – Lorentzian resonant wavelength, [m]

ε_h – permittivity of the host media

ω – frequency, [rad/s]

$E(t)$ – *external electric field function*, [V/m]

$P_{ij}(t)$ – *polarization function of transition ij* – is normalized by ε_0, $P_{ij}=P_{ij}[\mathrm{C/m^2}]\,/\,\varepsilon_0$

$N_j(t)$ – *population density function of j-th level* – is normalized by the total population density N_{tot}, $N_j=N_j[\mathrm{m}^{-3}]\,/\,N_{tot}$

$N_{ij}(t)=N_i(t)-N_j(t)$ – *population difference function*

$\hat{f}(\omega)=\int_{-\infty}^{\infty}f(t)e^{\imath\omega t}dt$ – the Fourier transform of time-domain function $f(t)$, $\left(f(t)=0,\,t<0\right)$

$\chi_{ij}(\omega)=\hat{P}_{ij}(\omega)\,/\,\hat{E}(\omega)$ – frequency domain susceptibility (time range for FFT is cropped either for probe or pump pulse)

A_{X}, σ_{X}, ω_{X}, $t_{0,\mathrm{X}}$, $\mathrm{X}\in\{\mathrm{pump},\,\mathrm{probe}\}$ – amplitude [V/m], Gaussian halfwidth [s], carrier frequency [rad/s], center [s] of pump and probe Gaussian pulses

ODE – ordinary differential equation

FWHM – full width at half maximum (calculated by intensity rather than by the field, $\mathrm{FWHM}=2\sigma\sqrt{\log 2}$)

INTRODUCTION

This document is a description of **PhotonicsGAIN-0D** simulation tool, which is staged at nanoHUB (www.nanoHUB.org) and provides time-domain simulation of 4-level atomic gain system and post-processing analyses of the amplification level. The tool adds to the collection of our other **nanophotonics tools** at nanoHUB [1-6]: **PhotonicsDB** – the material database of optical properties of various materials, **PhotonicsRT** –simulates planar nanostructured lamellar photonic crystals and non-reflecting coatings, **PhotonicsSHA-2D** – simulates cascaded photonic or plasmonic 2D metamaterials, **PhotonicsCL** – simulates cylindrical transformation optics lenses, **Hyperlens Layer Designer** and **Hyperlens Design Solver** – simulate cylindrical hyperlenses. These tools deliver a cloud computing service, offering off-site simulations done through standard web browsers, with demand for neither any powerful computational hardware nor any additional software installations. The hosting hardware and software platforms are provided by the Network for Computational Nanotechnology (NCN) at the Birck Nanotechnology Center at Purdue University. Along with the scientific simulation services, nanoHUB's cloud computing services also include courses, software tutorials, discussion groups and Internet-based infrastructure for effective collaboration in the major areas of nanoelectronics, nanoelectromechanical systems, and their application to nano-biosystems.

The development of the PhotonicsGAIN-0D solver has been motivated by the problem of achieving loss compensation in plasmonic elements of optical metamaterials. A recent approach to solve this problem is to introduce organic dye inclusions to a dielectric host of the metamaterial structure [7-17], and use light amplification based on the stimulated radiation emission from the dye-doped host, a phenomenon broadly used in laser science [18].

The amplification principle is based on getting pumped the laser media, which on certain conditions will emit photons on relaxation. A gain medium (or a dye-dopped host) is formalized as a quantum mechanical system of "atoms" (here, a general term for any atoms, molecules, ions, or instances of semiconducting crystal). The pumping process excites the atoms into higher quantum-mechanical energy levels. Then, for laser action to occur, the pumping process must produce *the population inversion*, e. g. more atoms must be excited into some higher i -th quantum energy level (E_i) than there are in some lower j -th energy level (E_j) in the laser medium. Once the population inversion of levels i, j is obtained, electromagnetic radiation within a certain narrow band of frequencies (near the frequency of the inverted transition $\omega_{ij} = (E_i - E_j) / \hbar$) can be coherently amplified, when going through the thick enough slab of the gain medium (in lasers the signal goes back and forth between the mirrors).

In this tool instead of modeling full-wave pulse propagation through a gain medium we study the local response (at fixed spatial point) of the gain medium to a given external time-dependent electric field – we calculate the population kinetics on all energy levels (pumping process, inversion, and then relaxation) and the effective frequency domain polarizability (susceptibility). The tool helps to study, verify, and optimize a simplified 4-level atomic model of a gain media.

In fact, real gain systems may involve a large number of energy levels, but many of them can be simplified to the four-level atomic system with similar essential features and qualitative behavior. For this reason we hope that the tool is helpful for different application of gain media beyond active metamaterials, e.g. in organic dye lasers, and organic dye spectroscopy.

In sections below we list notations and acronyms used in the document and GUI of the tool, and then give a detailed description of the four-level atomic system, simulated by the tool. All the simulation examples were performed for the 4-level gain system of Rhodamine800 dye. Parameters of this system were found by fitting simulation results to pump-probe experiment in [15], and they are set by default in the GUI of the tool.

For guidance on how to use the GUI of the tool please refer to our video tutorial.

4-LEVEL ATOMIC SYSTEM MODEL

We assume that the atomic system has 4 energy levels (fig. 1). The zero-th level is the ground level hosting the total population of the non-excited system. In our model the ground level atoms can be pumped with an external electric field to the highest level E_3 . Then on certain conditions on relaxation times (e.g. the relaxation time of 32 transition must be smaller than that of 21 and 30 transitions) the pumped system will get an inversion of levels E_2 sand E_1, between which the lasing action is intended to take place.

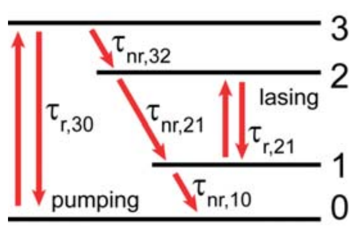

Figure 1. An energy transition diagram of the four level atomic system.

The system relaxes exponentially, following the Boltzmann principle. And we assume that initially the system is not excited – all the population is at the ground level. Thus, if $N_i(t)$ is the relative population density function of time at level E_i, then the population kinetics of entire system shown in fig. 1 satisfies the following system of equations

$$\begin{cases} N_3' &= -\tau_{32}^{-1}N_3 & & + f_{30} \\ N_2' &= -\tau_{21}^{-1}N_2 & + \tau_{32}^{-1}N_3 & + f_{21} \\ N_1' &= -\tau_{10}^{-1}N_1 & + \tau_{21}^{-1}N_2 & - f_{21} \, , \ t > 0 \, . \\ N_0' &= & \tau_{10}^{-1}N_1 & - f_{30} \\ N_0(0) = 1; N_1(0) = N_2(0) = N_3(0) = 0 \end{cases} \tag{1}$$

The first right hand side column defines the exponential relaxation of the upper level to the lower level with the total decay time τ_{ij} for each ij-transition. The second column is the inflow to the lower level produced by the relaxation of the upper level. The third column integrates the radiative transitions of the levels population stimulated by the external electric field. The total population $N_0(t) + N_1(t) + N_2(t) + N_3(t) = 1$ is always conserved.

Generally speaking the total decay time of each transition has radiative and non-radiative part $\tau_{ij} = (\tau_{\mathrm{r},ij}^{-1} + \tau_{\mathrm{nr},ij}^{-1})^{-1}$. In this model we assume that only transitions 30 and 21 have radiative part, and the non-radiative part of the transition 30 is neglected (fig. 1).

The driving terms f_{ij} stimulated by the external electric field $E(t)$ are given as

$$f_{ij} = \eta_{ij} E\left[P_{ij}' + \tfrac{1}{2}\Gamma_{ij} P_{ij}\right], \quad ij \in \{21, 30\}, \tag{2}$$

where $\eta_{ij} = \varepsilon_0 / (N_{tot}\hbar\omega_{ij})$; ω_{ij}, Γ_{ij}, P_{ij} are Lorentzian frequency, damping constant, and polarization of the transition. In the GUI we provide setting wavelength rather than the frequency, so that $\lambda_{ij} = 2\pi c / \omega_{ij}$. Each polarization $P_{ij}(t)$ satisfies the Lorentz ODE,

$$P_{ij}'' + \Gamma_{ij} P_{ij}' + \omega_{ij}^2 P_{ij} = \kappa_{ij}\left[N_j - N_i\right]\left[E + \nu_{ij} E'\right], \; ij \in \{30, 21\} \tag{3}$$

with an additional term ($\nu_{ij} E'$) defining a phase-shift in response, and the entire excitation term being proportional to the difference in populations. Here the coupling coefficients are $\kappa_{ij} = 6\pi N_{tot} c^3 / (\tau_{\mathrm{r},ij}\omega_{ij}^2 \sqrt{\varepsilon_{\mathrm{h}}})$, $\nu_{ij} = 2\sin\phi_{ij} / (\Gamma_{ij}\sin\phi_{ij} - \sqrt{4\omega_{ij}^2 - \Gamma_{ij}^2}\cos\phi_{ij})$, and ε_h is the permittivity of the host media. If the phase ϕ_{ij} is zero then $\nu_{ij} = 0$ and we get the classical Lorentz oscillator model. By adding a nonzero phase ϕ_{ij} we add non-symmetry to the Lorenzian line shape in frequency domain. In time domain this corresponds to the same damping oscillator but with a shift. So that in the assumption of constant population difference $N_{ij} = N_i - N_j$ we have $\chi_{ij}(t) = A_{ij} e^{-\Gamma_{ij} t}\sin(\omega_{ij} t - \phi_{ij})$, $A_{ij} = \kappa_{ij} N_{ij}\left(\omega_{ij}^2 - \Gamma_{ij}^2/4\right)^{-1/2}$. The susceptibility χ_{ij} is defined in frequency domain as $\chi_{ij}(\omega) = \hat{P}_{ij}(\omega) / \hat{E}(\omega)$.

EXTERNAL FIELD AND PUMP-PROBING

In the absence of the external electric field, the polarizations $P_{ij}(t)$ and driving terms $f_{ij}(t)$ are equal to zero, and the gain system stays in the initial equilibrium non-excited state.

In order to pump the gain system and get the population inversion of the lasing transition 21, the external field must start with a pumping pulse with high enough power (the pulse spectrum is usually a close proximity of a frequency ω_{30}). Besides the intensity of the external field, the excited polarization P_{30}, and therefore the driving term f_{30}, are proportional also to the population difference $(N_0 - N_3)$ at a given time, see eq. (1-3). So that the population difference determines the strength and the direction of the induced flow of population f_{30} between levels E_3 and E_0. Positive f_{30} means transition to higher energy level and is accompanied with the absorption of the external field, while negative f_{30} means population relaxation to ground level and is followed by emission. Typically, because of fast non-radiative relaxations and slow transition 30, population difference $(N_0 - N_3)$ stays positive in the applied external field or it reaches zero in case of high power of the applied field. However, shorter pulses in combination with high intensity of the external field may lead to $N_3 > N_0$. In this situation populations N_0 and N_3 will fall into alternate behavior and the transition 30 will absorb and re-emit photons in a cycle for some time (Rabi oscillations), see fig. 2c for an example.

After the gain system has been pumped, the relaxation time of the whole system is determined by the non-radiative lifetime of the lasing transition, which is usually the slowest non-radiative lifetime in the system (e.g. it is of the order of 0.1 ns for Rhodamine800 [15]). Before the inversion of the lasing transition relaxes, we set a probing pulse to estimate the amplification of the gain system (typical delay between pump and probe for Rhodamine800 experiment [15] was 50 ps). The probe pulse is usually several orders weaker than the pump pulse and its spectrum is usually a vicinity of the lasing frequency ω_{21}. As opposed to pump transition, the sign of the population difference $(N_1 - N_2)$ is negative for a pumped system and is reaching zero otherwise. So that maximum inversion will provide maximum emission, and in case if inversion is insufficient the probe pulse will be entirely absorbed by the pumping transition.

To estimate amplification/absorption of the pump and probe pulse we calculate efficient susceptibility $\chi_{ij}(\omega)$ for each pump and probe part of the pulse and polarizations. The susceptibility is defined in frequency domain as $\chi_{ij}(\omega) = \mathrm{FFT}\left(P_{ij}\big|_{[t_1,t_2]}\right) / \mathrm{FFT}\left(E\big|_{[t_1,t_2]}\right)$, where FFT means the Fast Fourier Transform of a time domain function, and $[t_1,t_2]$ is time range corresponding to pump or probe pulse. The analytical estimate of the susceptibility can be made from eq. (3) by assuming $N_0 - N_3 = 1$ (maximum absorption) and $N_1 - N_2 = -1$ (maximum emission)

$$\chi_{ij}(\omega) \approx \frac{\kappa_{ij} n_{ij}\left[1 - \iota\omega\nu_{ij}\right]}{-\omega^2 - \iota\omega\Gamma_{ij} + \omega_{ij}^2} \quad ij \in \{30,21\},\ n_{30} = 1,\ n_{21} = -1,\ ij \in \{30,21\}\,. \tag{4}$$

Note that the ideal analytical absorption level can be practically reached for transition 30 for the unsaturated system. However, the practical inversion rate $N_2 - N_1$ that can be reached by pumping process is usually far away from 100% (about 50% for Rhodamine800 [15]), and so it's normal that the practical emission rate is half less than its analytical estimation.

In the GUI we assume both pump and probe pulses to be Gaussian

$$E(t) = \sum_{\mathrm{i=pump,\ probe}} A_i \exp\{-(t - t_{0,i})^2 / 2\sigma_i^2\} \sin\omega_i t \quad (t_{0,\mathrm{pump}} < t_{0,\mathrm{probe}})\,. \tag{5}$$

SIMULATION EXAMPLE OF RH800

The parameters of the four-level gain system of Rhodamine800 dye in a solid host [15] are set by default in the GUI of the tool. We start from investigating the parameters of the pumping pulse. The gain system could be pumped with a shorter or longer pulse, but the power shall be enough to get the inversion of the lasing transition. On figure 1 we show an example of pumping process for gain system [15] using 100-fs (FWHM of the intensity, i.e. $\mathrm{FWHM}{=}\sigma 2\sqrt{\log 2}$) and 2-ps pumping pulses with (a) low power, which only slightly affects the populations, (b) medium power, sufficient to get a visible inversion of levels 2, 1 (c) high power which shows the behavior of the saturated system. The intensities for 2-ps pulse are scaled down to preserve the same power level as in (a)-(c) cases for the shorter, 100-fs pulse. This simulation helps to estimate the power required to get the inversion and to compare inversion rates for short and long pulses in a given gain system, see fig. 2. As discussed in the previous section, for short and intensive pump pulse (100-fs, 3e9 V/m) Rabi oscillations occur in this gain system.

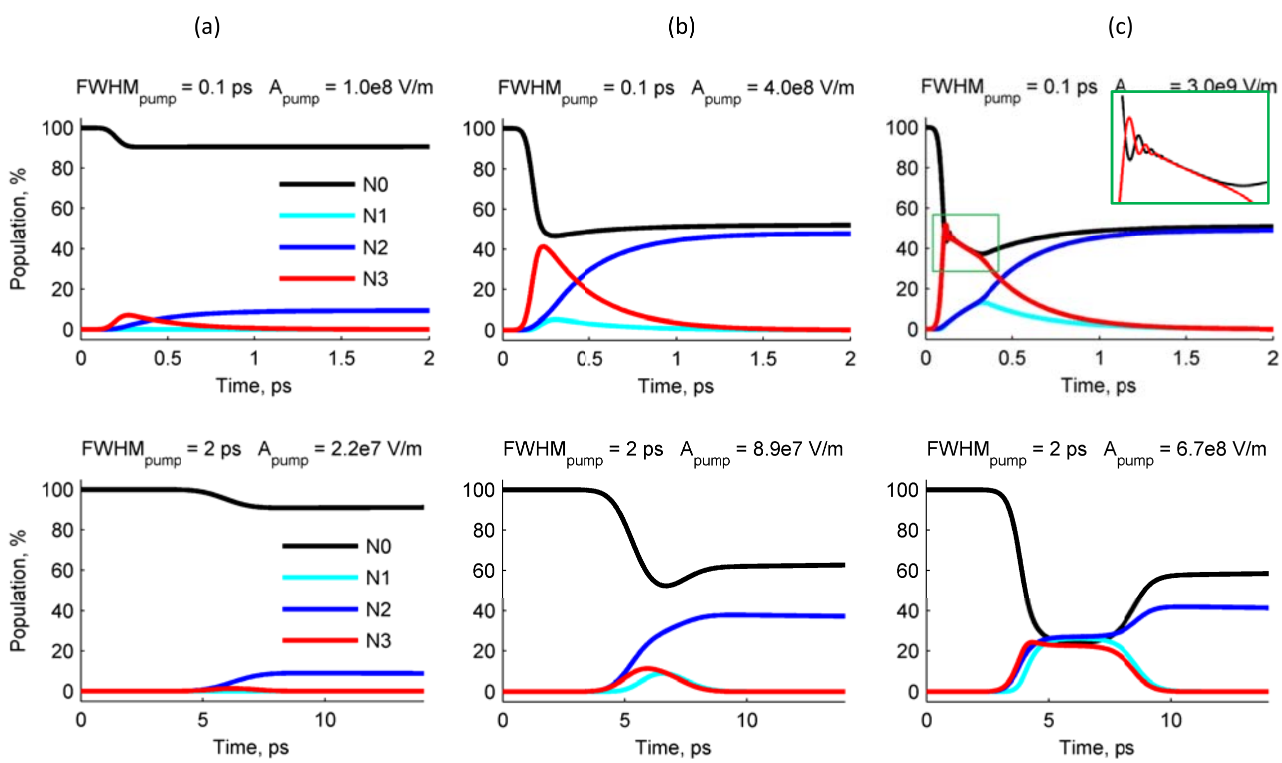

Figure 2. Pumping process for a gain system of Rhodamine 800 dye [15] for different pulse durations and intensities. Upper panel σ_{pump} = 100 fs pulse, (a) $A_{pump} = 10^8$ (b) $A_{pump} = 4\times10^8$ (c) $A_{pump} = 3\times10^9$. Lower panel σ_{pump} = 2 ps pulse, (a) $A_{pump} = 2.2\times10^7$ (b) $A_{pump} = 8.9\times10^7$ (c) $A_{pump} = 6.7\times10^8$

Once the parameters of pumping pulse are set, then the amplification of the probe signal can be examined by plotting the imaginary part of the frequency domain susceptibility. In figure 3 we plot imaginary part of χ_{30}, χ_{21} susceptibilities as well as of the resulting sum $\chi_{30} + \chi_{21}$ for the probe pulse (FWHM = 5fs, 1e6 V/m) and for three variants of pumping process (a), (b), (c) from fig. 2. Dotted color-matched lines in fig. 3 are matching analytical estimates of susceptibilities, eq. (4). As predicted in the previous section, if the gain system is insufficiently pumped (fig. 3a) then absorption is close to its analytical estimation and $\operatorname{Im}\chi_{30} > 0$ dominates versus the small emission $\operatorname{Im}\chi_{21} < 0$, so that the resulting response $\chi_{30} + \chi_{21}$ has absorption in the entire range. As the 30 absorber becomes saturated (fig. 3bc) the absorption lineshape follows no more the analytical absorption estimation with a constant population difference. By the same time, the emission becomes sufficiently stronger than in case (a), so that the resulting response (black line) has emission in the entire shown range. The deviation of the emission from the its analytical estimate (4) is explained by incomplete inversion of populations $N_2 - N_1$, see fig.2c. The difference between fig.3b and fig.3c is insufficient – the latter has only slightly larger emission rate and even less noticeable reduction in the absorption peak.

(a) (b) (c)

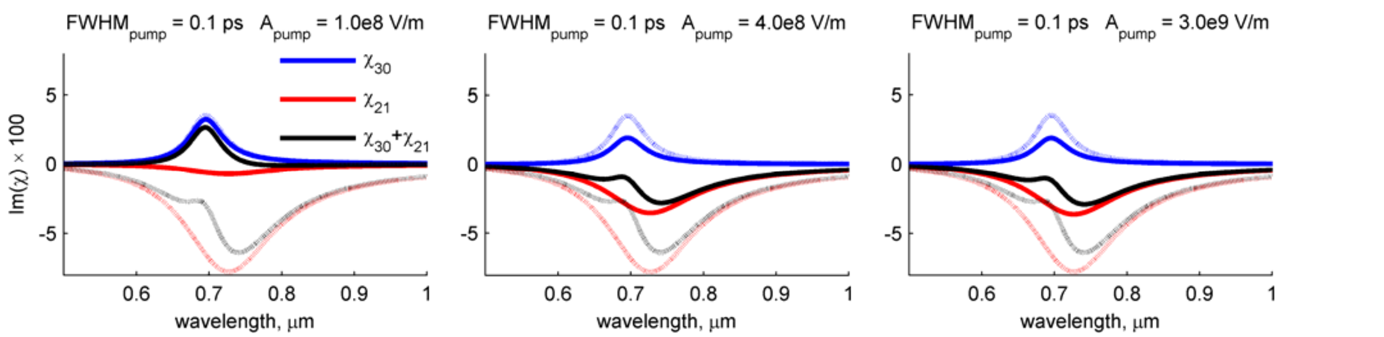

Figure 3. Imaginary part of frequency domain susceptibility of the probe pulse for three pumping processes (see fig.2). The dotted lines show analytical estimates, as in eq. (4). The resulting sum (black line) demonstrates emission for cases (b-c), while in case (a) the probe pulse is absorbed by pumping transition 30.

For more information please refer to our online tutorial.

REFERENCES

[1] Ni, X. et al., "PhotonicsDB: Optical Constants," http://nanohub.org/resources/photonicscdb, doi: 10254/nanohub-r3692.6, 2008.

[2] Ishii, S. et al., "PhotonicsRT: Wave Propagation in Multilayer Structures," http://nanohub.org/resources/photonicscrt, doi: 10254/nanohub-r5968.14, 2008.

[3] Ni, X. et al., "PhotonicsSHA-2D: Modeling of Single-Period Multilayer Optical Gratings and Metamaterials," http://nanohub.org/resources/sha2d, doi: 10254/nanohub-r6977.6, 2009.

[4] Swanson, M. et al., "Hyperlens Layer Designer," http://nanohub.org/resources/hypiedesigner, doi: 10254/nanohub-r4703.1, 2008.

[5] Swanson, M. et al., "Hyperlens Design Solver," http://nanohub.org/resources/hypiesolver, doi: 10254/nanohub-r4770.2, 2008.

[6] Ni, X. et al. "PhotonicsCL: Photonic Cylindrical Multilayer Lenses," http://nanohub.org/resources/photonicscl, doi: 10254/nanohub-r9914.3.

[7] Stockman, M. I., "The spaser as a nanoscale quantum generator and ultrafast amplifier," J. Opt., Vol. 12, 024004, 2010.

[8] Noginov, M. A. Zhu, G., Bahoura, G. M., Adegoke, J., Small, C. E., Ritzo, B. A., Drachev, V. P. and Shalaev, V. M., "Enhancement of surface plasmons in an Ag aggregate by optical gain in a dielectric medium," Opt. Lett., Vol. 31, 3022-3024, 2006.

[9] Zheludev, N. I., Prosvirnin, S. L., Papasimakis, N. and Fedotov, V. A., "Lasing spaser," Nat. Photonics, Vol. 2, 351-354, 2008.

[10] Plum, E., Fedotov, V. A., Kuo, P., Tsai, D. P. and Zheludev, N. I., "Towards the lasing spaser: controlling metamaterial optical response with semiconductor quantum dots," Opt. Exp., Vol. 17, 8548-8551, 2009.

[11] Sarychev, A. K. and Tartakovsky, G., "Magnetic plasmonic metamaterials in actively pumped host medium and plasmonic nanolaser," Phys. Rev. B, Vol. 75, 085436, 2007.

[12] Xiao, S. M., Drachev, V. P., Kildishev, A. V., Ni, X. J., Chettiar, U. K., Yuan, H. K. and Shalaev, V. M., “Loss-free and active optical negative-index metamaterials,” Nature, Vol. 466, 735-U6, 2010.

[13] Fang, A., Koschny, Th., Wegener, M. and Soukoulis, C. M., “Self-consistent calculation of metamaterial with gain,” Phys. Rev. B, Vol. 79, 241104, 2009.

[14] Wuestner, S., Pusch, A., Tsakmakidis, K.L., Hamm, J. M. and Hess, O., “Gain and plasmon dynamics in active negative-index metamaterials,” Phil. Trans. R. Soc. A, Vol. 369, 3525-3550, 2011.

[15] Trieschmann, J., Xiao, S., Prokopeva, L. J., Drachev, V. P. and Kildishev, A. V., “Experimental retrieval of the kinetic parameters of a dye in a solid film,” Opt. Express, Vol. 19, 18253-18259, 2011.

[16] Prokopeva, L. J., Trieschmann, J., Klar, T. A. and Kildishev, A. V., “Numerical modeling of active plasmonic metamaterials,” Proc. SPIE, Vol. 8172, 81720B, 2011.

[17] Bahaa E. A. Saleh, Malvin Carl Teich, Fundamentals of photonics (Wiley-Interscience, 2007).

[18] Siegman, A. E., Lasers (University Science Books, 1986).

[19] Boyd, R. W., Nonlinear Optics (Academic Press, 2008).